Hedgehog Buckyball: A High-Symmetry Complete Polyhedral Oligomeric Silsesquioxane (POSS)

Yu Hu [1],*, You Wang [1],*, Hong You [2] and Di Wang [3]

1   School of Materials Science and Engineering, Harbin Institute of Technology, Harbin 150001, China
2   State Key Laboratory of Urban Water Resource and Environment, Harbin Institute of Technology, Harbin 150001, China; youhong@hit.edu.cn
3   Material Science and Engineering College, Northeast Forestry University, Harbin 150040, China; diwang1030@126.com
*   Correspondence: yuhu0104@hit.edu.cn (Y.H.); y-wang@hit.edu.cn (Y.W.); Tel.: +86-451-8641-2679 (Y.H.); +86-451-8641-2516 (Y.W.)

Abstract: In this study, we report UV-MALDI-TOF MS evidence of a fullerene-like silsesquioxane, a high-symmetry polyhedral oligomeric silsesquioxane (POSS or SSO) formulated as R_{60}-$Si_{60}O_{90}$ or T_{60} (T = $RSiO_{1.5}$). The T_{60} preparation can be performed using a normal hydrolytic condensation of [(3-methacryloxy)propyl]trimethoxysilane (MPMS) as an example. Theoretically, four $3sp^3$ hybrid orbitals (each containing an unpaired electron) of a Si atom are generated before the bond formation. Then it bonds to another four atom electrons using the four generated hybrid orbitals which produced a stable configuration. This fullerene-like silsesquioxane should exhibit much more functionality, activity and selectivity and is easier to assemble than the double bonds in a fullerene.

Keywords: polyhedral oligomeric silsesquioxane (POSS); high-symmetry; fullerene-like silsesquioxane; synthesis and characterization

The fullerene buckyball (FBB), C_{60}, was named "Molecule of the Year" for 1991 by Science [1]. Since the discovery of the C_{60} buckyball, fullerene science has continued to accelerate, investigating both the basic science and its potential applications [2,3]. One investigation involves a major focus on its analogue, the Si_{60} cluster [4,5]. For Si_{60} clusters, the cages should not be very stable due to the use of three ($3sp^3$) orbitals to bond to other Si atoms. Thus, the cages need some other atoms for the fourth bond whereas the C_{60} fullerene uses the second period sp^2 orbitals along with a π bond to bond exclusively with other C atoms. Most investigations focus on endohedral Si_{60} isomers (using the fourth bond of the $3sp^3$ orbital) which are unstable [6]. To produce a stable Si_{60} configuration, Wang and Yang conducted ab initio calculations based on density functional theory on a Si_{60} fullerene-like cage passivated with F or Cl atoms [7]; however, this research is limited by a complex experimental synthesis.

In this study, we report UV-MALDI-TOF MS evidence of a fullerene-like silsesquioxane, a high-symmetry polyhedral oligomeric silsesquioxane (POSS or SSO) formulated as R_{60}-$Si_{60}O_{90}$ or T_{60} (T = $RSiO_{1.5}$) [8]. Theoretically, four $3sp^3$ hybrid orbitals (each containing an unpaired electron) of a Si atom are generated before the bond formation. Then it bonds to another four atom electrons using the four generated hybrid orbitals which produced a stable configuration. A significant difference between a FBB and T_{60} POSS is that the cage in the former is the four-bond (three $2sp^2$ hybrid orbits and one original 2p orbital) connection of each C atom on the FBB surface, while it is the three-bond (three of four $3sp^3$ hybrid orbits) connection of each Si atom on the POSS surface. The remaining bond to each silicon connects to a pendant organic group adorning the surface of the T_{60} cage, showing a hedgehog buckyball (HBB, see Figure 1). These organic groups exhibit much more functionality, activity and

selectivity and are easier to assemble than the double bonds in a fullerene, which facilitates the synthesis of POSS-based materials possessing unique properties and the ability to set up applications [9–14].
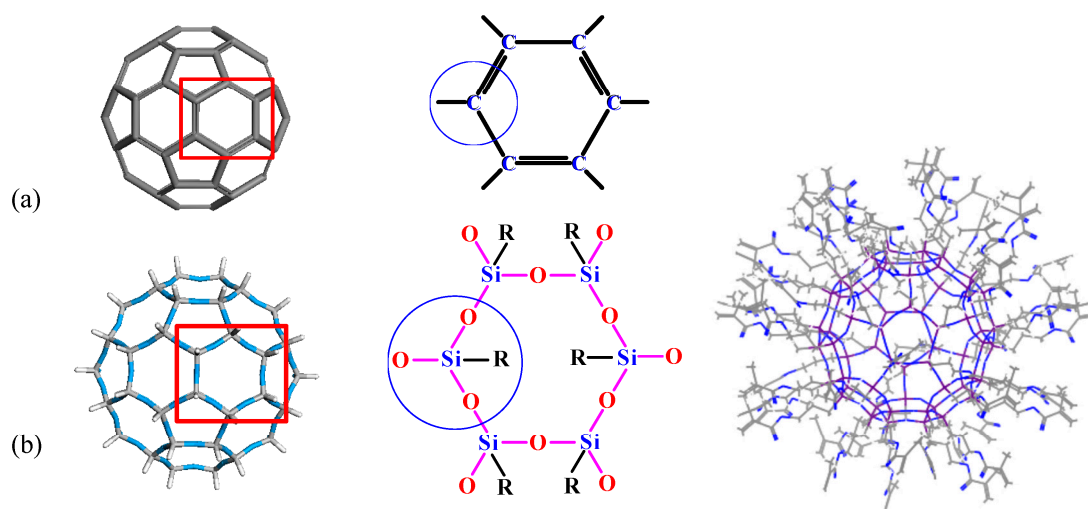

Figure 1. The molecular structures: (**a**) FBB, the C atom on the FBB surface connects the other three C atoms; (**b**) HBB, the Si atom connects the bridged three O atoms on the T_{60} surface and one organic group R outside the HBB surface.

The HBB T_{60} preparation can be performed using a normal hydrolytic condensation of [(3-methacryloxy)propyl]trimethoxysilane (MPMS) that we have used to prepare silsesquioxane coatings [15,16]. Hydrolysis and condensation normally give rise to smaller oligomers with a dozen or fewer monomers interconnected into rings [17]. By extending the condensation time we are able to produce more viscous products (M-POSS or MSSO) with molecular weights in the range calculated for methacryloxypropy-T_{60} (10,755 Daltons).

Generally the groups and the location of the groups are determined by FTIR and NMR (^{1}H, ^{13}C and ^{29}Si); then all possible predicted structures are established by the molecular weights assigned from the peaks of UVMALDI-TOF MS and the general formula [8,18,19]. Figure S1 schemes the structural formula of MSSO, facilitating analysis and assignment of FTIR and ^{1}H- and ^{13}C-NMR spectra. The typical FTIR MSSO spectrum (Figure S2b) bands at 417–478 and 1122–1129 cm^{-1} are primarily ascribed to the stretching of O–Si–O and Si–O–Si; the obvious bands at about 1298, 1410 and 1724 cm^{-1} derive from stretches of CH=CH$_2$ and C=O groups in methacrylate chains; a decrease in the intensity of the Si–OCH$_3$ group band at 2938 cm^{-1} is observed relative to the lower molecular weight MSSO, evidenced together with the generation of a broad band at 3423 cm^{-1}, assigned to –OH groups from Si–OH. Except for bands at 2938 and 3423 cm^{-1}, these data are in good agreement with those of the MPMS spectrum in Figure S2a and give complementary information for the characterization of the structure.

The following peaks in the ^{1}H-NMR spectrum (Figure S3) were assigned: 0.698 ppm (1); 1.784 ppm (2); 1.925 ppm (7); 3.520, 3.580 ppm (CH$_3$–OH, Si–OH); 4.111, 4.103 ppm (3); 5.545, 6.091 ppm (5, 6); 7.280 ppm (CHCl$_3$); 8.004, 8.049 ppm (HCOOCH$_3$, HCOOH). The following peaks in the ^{13}C-NMR spectrum (Figure S4) were assigned: 8.534 ppm (1); 17.865 ppm (7); 21.954 ppm (2); 66.121, 65.894 ppm (3); 76.674, 77.000, 77.319 ppm (CHCl$_3$, CH$_3$-OH, Si–OH); 125.006 ppm (5); 135.983 ppm (6); 162.785 ppm (HCOOH); 167.019 ppm (4, HCOOCH$_3$). Besides ^{1}H- and ^{13}C-NMR spectroscopy, ^{29}Si NMR spectroscopy permits quantitative measurement of the degree of condensation by the relative abundance of the T^3 silicon nuclei, Si–(O–Si)$_3$ [20–23]: −65.681 ppm is characteristic of the T^3 species, and −56.577 ppm can be assigned to T^2 structures, Si–(O–Si)$_2$(OH), from incompletely condensed species in the product mixture; no T^0 or T^1 structures were present in the ^{29}Si-NMR spectrum which is consistent with higher molecular weight and cyclic MSSO.

Figure 2 shows the UV-MALDI-TOF MS in the m/z = 0–11,000 Da range corresponding to MSSO molecules. Three high-symmetry complete MSSOs, T_8, T_{20} and T_{60} (see Figure 3), were assigned (see Table 1). These predicted structures have a compliance between the experimental measurement value and the calculated molecular weight according to ion adducts (M_w + H$^+$ or M_w + Na$^+$ or M_w + K$^+$) [24], however, there are still few differences, probably from ion adducts selected, solvent used for the measurement operation, calculations and so on. T_{60}, one of three high-symmetry complete MSSOs, is a fullerene-like HBB and is denoted as MP-HBB as shown in Figure 3c. The difference between HBB and FBB (as mentioned above) provides an ideal vehicle for exciting research which will be timely, rapidly evolving, multidisciplinary and even appealing on an aesthetic level.
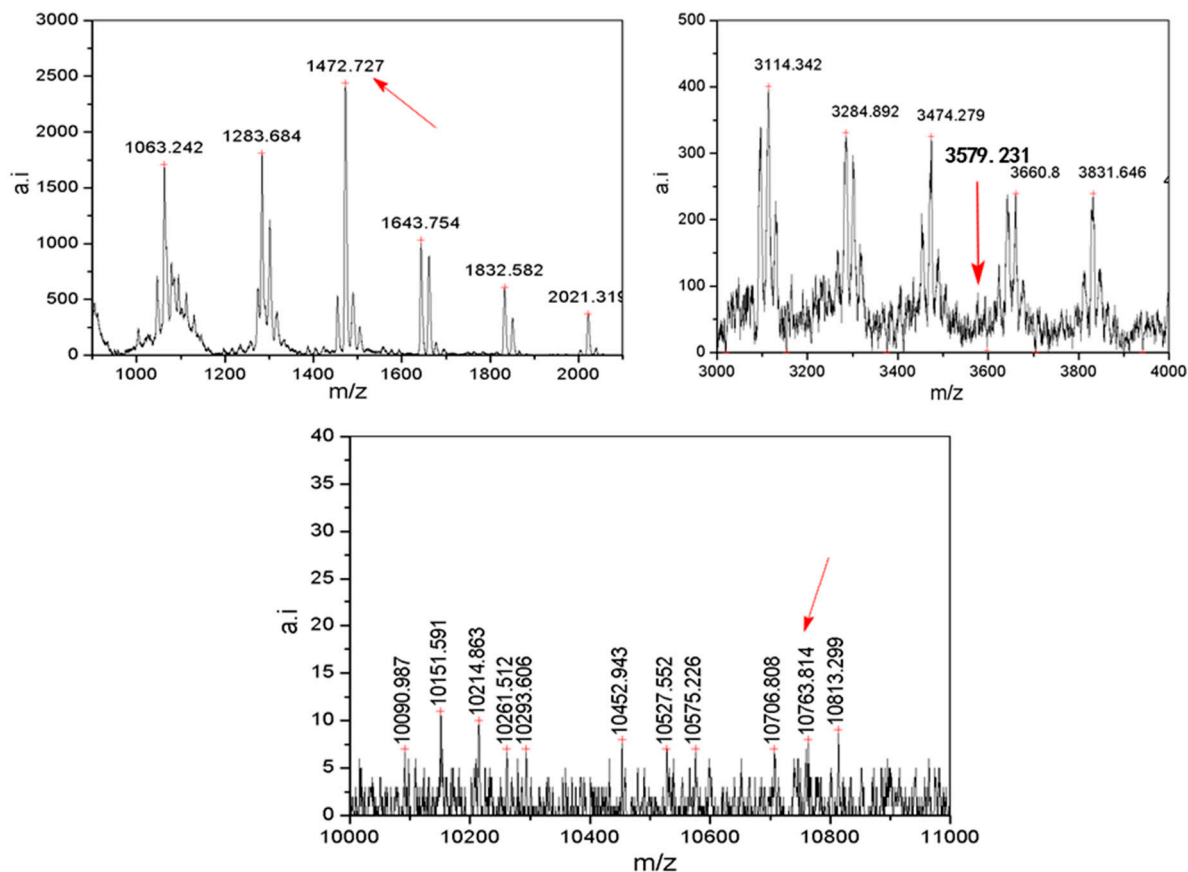
**Figure 2.** The UV-MALDI-TOF MS in the m/z = 500–11,000 Da range correspond to the MSSO oligomers.
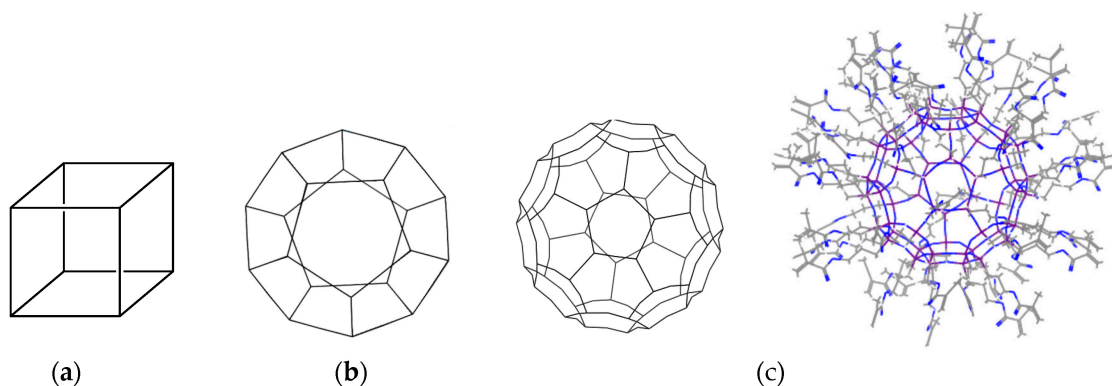
Figure 3. Structures of three high-symmetry complete MSSOs: (**a**) T_8; (**b**) T_{20} and (**c**) T_{60}.

Table 1. Three high-symmetry complete MSSOs assigned by the mass spectrum (m/z = 0–11,000 Da).

Experiment (m/z)	Assigned structure	Calculation (m/z) (+H$^+$, K$^+$)	Symmetry
1,472.73	$R_8Si_8O_{12}$ (+K$^+$)	1,472.98	O_h
3,579.23	$R_{20}Si_{20}O_{30}$ (+H$^+$)	3,585.96	I_h
10,763.81	$R_{60}Si_{60}O_{90}$ (+H$^+$)	10,755.88	I_h

Additional corroborating evidence for the proposed cyclic structures can be observed in the gel permeation chromatography (GPC) chromatograms obtained for the MSSO samples. Figure 4 shows the mass distribution of the MSSOs measured by a GPC device which provides refractive index data. The distribution profiles indicate that the oligomers are formed in three successive groups with average molecular weights of 1413.8, 4538.8 and 16,260.0 (see Figure 4b3, b2 and b1, respectively) corresponding to fractions containing the T_{60}, T_{20} and T_8 cyclic compounds [25].
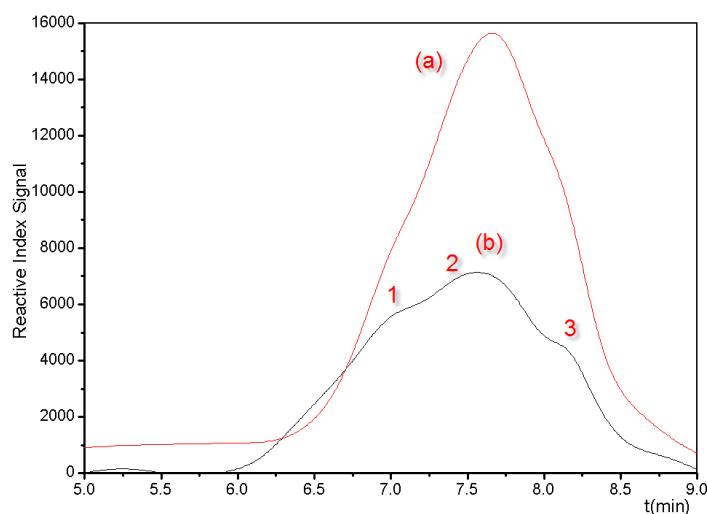
Figure 4. The mass distribution of the MSSO oligomers measured by a GPC device which provides refractive index data: (**a**) reaction under 70 °C for 12 days; (**b**) reaction under 35 °C for 20 days, average molecular weights of oligomers formed in three successive groups with (**b1**) 16,260.0, (**b2**) 4538.8 and (**b3**) 1413.8, corresponding to fractions containing the T_{60}, T_{20} and T_8 cyclic compounds.

Further research will be conducted on this MP-HBB to separate it from multiple MSSO structures using a gel permeation column. The intensity of the MP-T_{60} present can be determined by GPC or size exclusion chromatography (SEC), and the mass of the elutant is again measured by a mass spectrometer [25,26].

Author Contributions: You Wang and Hong You conceived and designed the project and experiments; Di Wang and Yu Hu performed the calculation, experiments and paper writing.

Conflicts of Interest: The authors declare no conflict of interest. The founding sponsors had no role in the design of the study; in the collection, analyses, or interpretation of data; in the writing of the manuscript, and in the decision to publish the results.

References

1. Koshland, D.E., Jr. Molecule of the Year. *Science* **1991**, *254*, 1705. [CrossRef] [PubMed]
2. Rao, A.; Wilson, M.W.B.; Hodgkiss, J.M.; Albert-Seifried, S.; Bassler, H.; Friend, R.H. Exciton fission and charge generation via triplet excitons in pentacene/C_{60} bilayers. *J. Am. Chem. Soc.* **2010**, *132*, 12698–12703. [CrossRef] [PubMed]
3. Geng, J.F.; Zhou, W.Z.; Skelton, P.; Yue, W.B.; Kinloch, I.A.; Windle, A.H.; Johnson, B.F.G. Crystal structure and growth mechanism of unusually long fullerene (C_{60}) nanowires. *J. Am. Chem. Soc.* **2008**, *130*, 2527–2534. [CrossRef] [PubMed]
4. Crespo, R.; Piqueras, M.C.; Tomás, F. Ab initio investigation of icosahedral Si-60. *Synth. Metal.* **1996**, *77*, 13–15. [CrossRef]
5. Yoo, S.; Zhao, J.; Wang, J.; Xiao, X.C. Endohedral Silicon Fullerenes Si_N ($27 \leq N \leq 39$). *J. Am. Chem. Soc.* **2004**, *126*, 13845–13849. [CrossRef] [PubMed]
6. Zhao, J.; Ma, L.; Wen, B. Lowest-energy endohedral fullerene structure of Si_{60} from a genetic algorithm and density-functional theory. *J. Phys. Cond. Matter* **2007**, *19*, 226208. [CrossRef]
7. Wang, L.; Yang, D. Si_{60} fullerene-like cage passivated by F and Cl. *Mol. Simul.* **2010**, *36*, 493–495. [CrossRef]
8. Eisenberg, P.; Erra-Balsells, R.; Ishikawa, Y.; Lucas, J.C.; Nonami, H.; Williams, R.J.J. Silsesquioxanes derived from the bulk polycondensation of [3-(methacryloxy)propyl]trimethoxysilane with concentrated formic acid: Evolution of molar mass distributions and fraction of intramolecular cycles. *Macromols* **2002**, *35*, 1160–1174. [CrossRef]
9. Hu, Y.; Geng, W.; You, H.; Wang, H.; Loy, D.A. Modification of a phenolic resin with epoxy- and methacrylate-functionalized silica sols to improve the ablation resistance of their glass fiber-reinforced composites. *Polymers* **2014**, *6*, 105–113. [CrossRef]
10. Mohamed, M.G.; Kuo, S. Polybenzoxazine/polyhedral oligomeric silsesquioxane (POSS) Nanocomposites. *Polymers* **2016**, *8*, 225–245. [CrossRef]
11. Wang, H.; Liu, L.; Huang, Y.; Wang, D.; Hu, L.; Loy, D.A. Enhancement corrosion resistance of (γ-glycidyloxypropyl)-silsesquioxane-titanium dioxide films and its validation by gas molecule diffusion Coefficients using molecular dynamics (MD) simulation. *Polymers* **2014**, *6*, 300–310. [CrossRef]
12. Blanco, I.; Abate, L.; Bottino, F.A.; Bottino, P. Thermal behaviour of a series of novel aliphatic bridged polyhedral oligomeric silsesquioxanes (POSSs)/polystyrene (PS) nanocomposites: The influence of the bridge length on the resistance to thermal degradation. *Polym. Degrad. Stab.* **2014**, *102*, 132–137. [CrossRef]
13. Jiang, D.W.; Liu, L.; Long, J.; Xing, L.X.; Huang, Y.D.; Wu, Z.J.; Yan, X.R.; Guo, Z.H. Reinforced unsaturated polyester composites by chemically grafting amino-POSS onto carbon fibers with active double spiral structural spiralphosphodichlor. *Compos. Sci. Technol.* **2014**, *100*, 158–165. [CrossRef]
14. Wu, G.S.; Ma, L.C.; Wang, Y.W.; Liu, L.; Huang, Y.D. Interfacial properties and impact toughness of methylphenylsilicone resin composites by chemically grafting POSS and tetraethylenepentamine onto carbon fibers. *Compos. A Appl. Sci. Manuf.* **2016**, *84*, 1–8. [CrossRef]
15. Wang, D.; Chen, X.; Zhang, X.; Liu, Y.; Hu, L. Enhancement corrosion resistance of (γ-methacryloxypropyl)-silsesquioxane hybrid films and its validation by gas-molecule diffusion coefficients using MD simulation. *J. Sol Gel Sci. Technol.* **2009**, *49*, 293–300. [CrossRef]
16. Zhang, X.; Hu, L.; Sun, D. Nanoindentation and nanoscratch profiles of hybrid films based on (γ-methacrylpropyl)trimethoxysilane and tetraethoxysilane. *Acta Mater.* **2006**, *54*, 5469–5475. [CrossRef]
17. Lichtenhan, J.D. Economic and commercialization of nanostructured hybrid chemicals. In *Organic/Inorganic Hybrid Materials*, 1st ed.; Blum, F.D., Laine, R.M., Eds.; ACS, Division of Polymer Chemistry: Washington, DC, USA, 2003; pp. 17–34.
18. Hu, L.; Zhao, S.; Liu, Z.; Sun, Y. Family of silsesquioxanes for coating II: Influence of condition on silsesquioxanes. In *Organic/Inorganic Hybrid Materials*, 1st ed.; Blum, F.D., Laine, R.M., Eds.; ACS, Division of Polymer Chemistry: Washington, DC, USA, 2003; pp. 343–347.
19. Wallace, W.E.; Guttman, C.M.; Antonucci, J.M. Polymeric silsesquioxanes: Degree-of-intramolecular -condensation measured by mass spectrometry. *Polymer* **2000**, *41*, 2219–2226. [CrossRef]
20. Wang, D.; You, H.; Hu, L. Study of three-dimensional configurations of (γ-methacryloxypropyl)-silsesquioxanes by ultraviolet laser matrix-assisted desorption/ionization time-of-flight mass spectrometry and quantum chemical calculation. *Rapid Commun. Mass Spectrom.* **2011**, *25*, 1652–1660. [CrossRef] [PubMed]

21. Romeo, H.E.; Fanovich, M.A.; Williams, R.J.J.; Matějka, L.; Pleštil, J.; Brus, J. Self-assembly of a bridged silsesquioxane containing a pendant hydrophobic chain in the organic bridge. *Macromols* **2007**, *40*, 1435–1443. [CrossRef]

22. Feher, F.J.; Wyndham, K.D. Amine and ester-substituted silsesquioxanes: Synthesis, characterization and use as a core for starburst dendrimers. *Chem. Commun.* **1998**, 323–324. [CrossRef]

23. Feher, F.J.; Soulivong, D.; Nguyen, F. Practical methods for synthesizing four incompletely condensed silsesquioxanes from a single $R_8Si_8O_{12}$ framework. *Chem. Commun.* **1998**, 1279–1280. [CrossRef]

24. Zhang, X.; Hu, L.; Sun, D.; Zhao, W. Study of three-dimensional configurations of organic/inorganic hybrid nanostructural blocks: A quantum chemical investigation for cage structure of (γ-glycidoxypropyl) silsesquioxanes. *J. Mol. Struct.* **2008**, *872*, 197–204. [CrossRef]

25. Bujalski, D.R.; Chen, H.; Tecklenburg, R.E.; Moyer, E.S.; Zank, G.A.; Su, K. Compositional and structural analysis of a compositional and structural analysis of a $(PhSiO_{3/2})_{0.35}(MeSiO_{3/2})_{0.40}(Me_2ViSiO_{1/2})_{0.25}$ resin. *Macromols* **2003**, *36*, 180–197. [CrossRef]

26. Eisenberg, P.; Erra-Balsells, R.; Ishikawa, Y.; Lucas, J.C.; Mauri, A.N.; Nonami, H.; Riccardi, C.C.; Williams, R.J.J. Cagelike precursors of HIGH-molar-mass silsesquioxanes formed by the hydrolytic condensation of trialkoxysilanes. *Macromols* **2000**, *33*, 1940–1947. [CrossRef]